Electronic Supplementary Information

A Three-dimensional origami-based Immuno-biofuel cell for Self-Powered, Low-cost, and Sensitive Point-of-care Testing

Yanhu Wang,[a] Lei Ge,[b] Panpan Wang,[a] Mei Yan,[a] Jinghua Yu,*[a] and Shenguang Ge[a]

Chemicals and Materials

Glucose dehydrogenase (GDH) from Thermoplasma acidophilum (E.C.1.1.1.47, 183 Umg^{-1}), bilirubin oxidase (BOD) from Myrothe-cium verrucaria (E.C.1.10.3.2, 6 Umg^{-1}), NAD^+/NADH, poly(diallyldimethylammonium chloride) (PDDA) and bovine serum albumin (BSA) were purchased from Sigma. Carbon nanotubes (CNTs) were purchased from Shenzhen Nanotech. Port. Co. Ltd. (Shenzhen, China) without further purification. Glucose was obtained from Beijing Chemical Reagent Company (Beijing, China). CEA, CEA antibodies, and GDH-labeled CEA were purchased from Linc-Bio Science Co. Ltd. (Shanghai, China). Whatman chromatography paper #1 (pure cellulose paper) was obtained from GE Healthcare Worldwide (Pudong Shanghai, China) and used with further adjustment of size (A4). Ultrapure water obtained from a Millipore water purification system (≥18 MU, Milli-Q, Millipore) was used in all assays and solutions. Blocking buffer for blocking the residual reactive sites on the antibody immobilized paper was pH 7.4 phosphate buffer solution (PBS) containing 0.5% BSA and 0.05% Tween. Tetrachloroauric acid ($HAuCl_4$) as the precursor for the formation of AuNP seeds and growth solution was purchased from Shanghai Sangon Biological Engineering Technology & Services Co. Potassium ferricyanide, $NaBH_4$, and sodium citrate were products from Shanghai Chemical Reagent Co. All other reagents were of analytical grade and used as received.

Preparation of the μPADs

The preparation of the μ-PADs was similarly to our previous work [3] with modifications and a detailed procedure was described below. Wax was used as the paper hydrophobization and insulation agent in this work to construct hydrophobic barrier on paper. The paper-based device (shown in scheme 1) was comprised of three layers of patterned rectangular papers with the same size (15.0 mm×15.0 mm), named as anodic tab (the red one), reservoir tab (the green one), and cathodic tab (the blue one) below. The microfluidic origami electronic device consisted of two unprinted line and three circular hydrophilic zones (6.0 mm in diameter, respectively). The unprinted line was defined as folding line, which could ensure that the hydrophilic zone on the microfluidic origami electronic device are properly and exactly aligned after folding. The circle hydrophilic zones were designed for screen-printing carbon electrode on anodic tab and cathodic tab, respectively. After baking the wax-patterned paper sheet in an oven at 130 ℃ for 150 s, the as-prepared sheet was ready for printing electrode after cooling to room temperature. The disk-like carbon electrodes (5.0 mm in diameter) were screen-printed onto the circle hydrophilic zones on anodic tab and cathodic tab, respectively (Scheme S1).

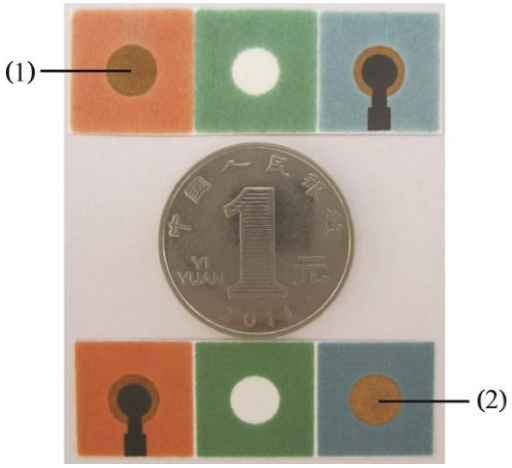

Scheme S1. Picture of this 3D-μ-OBFCAD. (1) Au-PCE, (2) Au-PAE.

Figure S1. Wax-printed 3D-μ-OBFCADs on a paper sheet (A4) before baking.

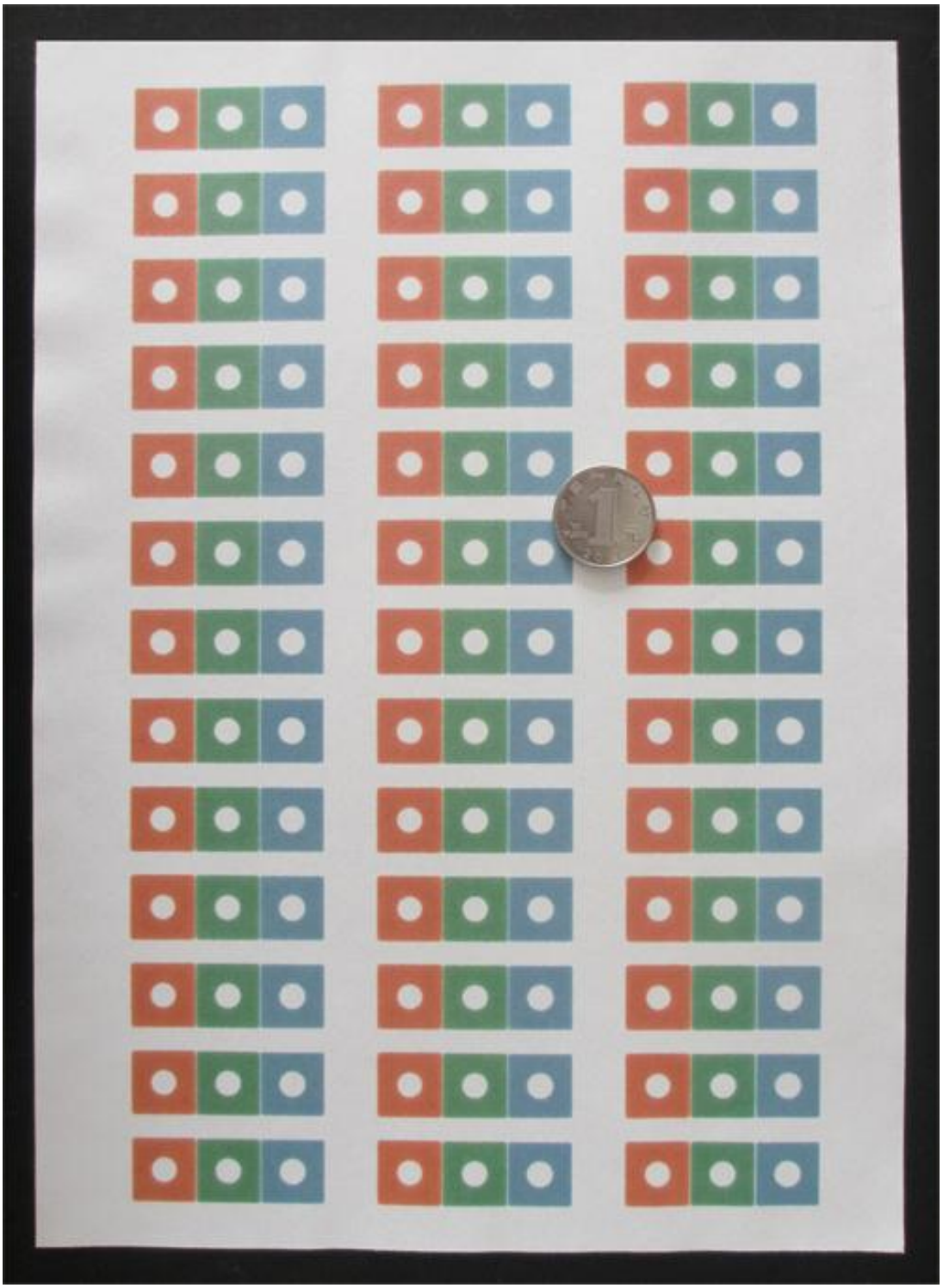

Figure S2. Right side of wax-printed 3D-μ-OBFCADs on a paper sheet (A4) after baking.

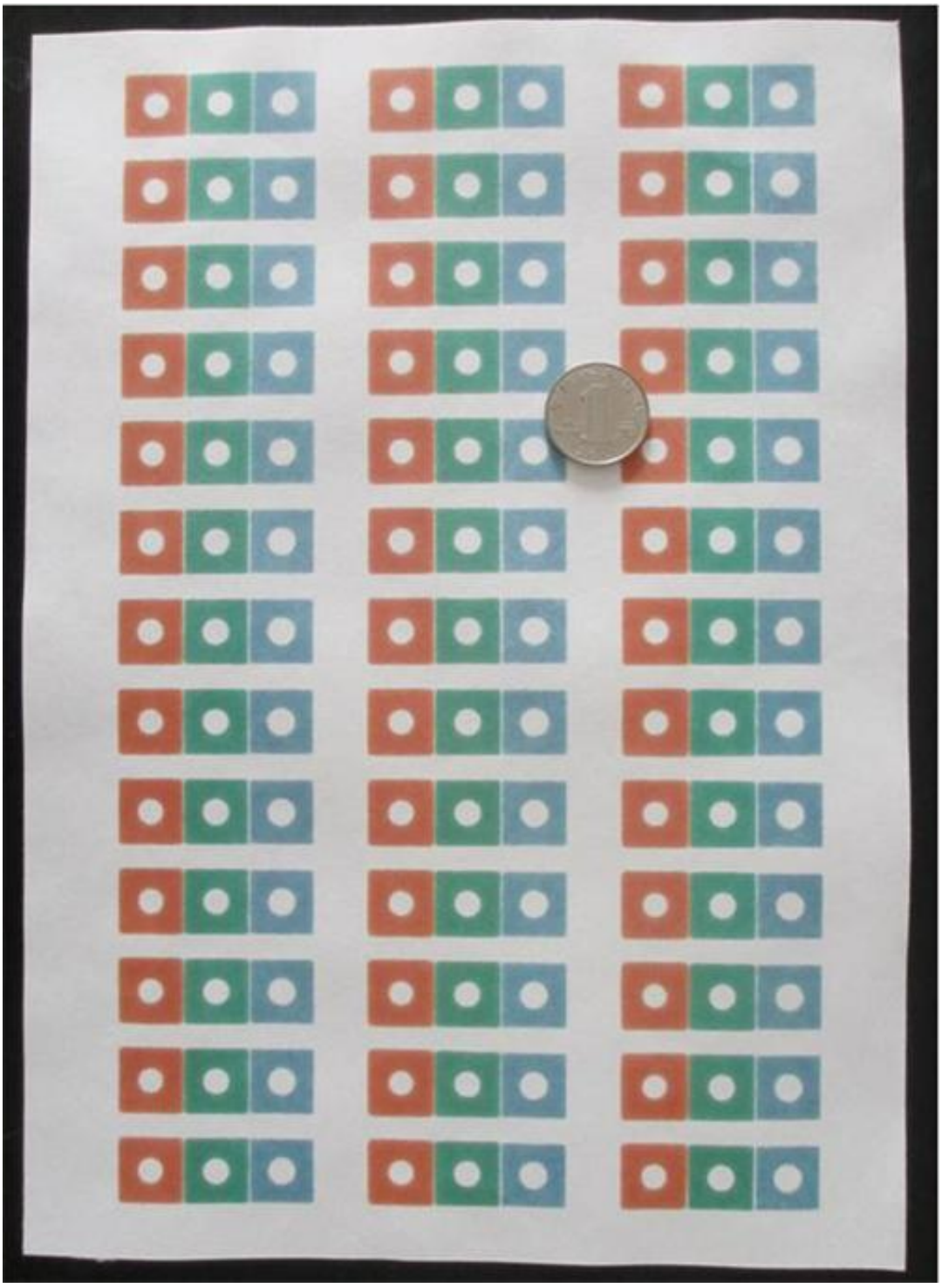

Figure S3. Reverse side of wax-printed 3D-μ-OBFCADs on a paper sheet (A4) after baking.

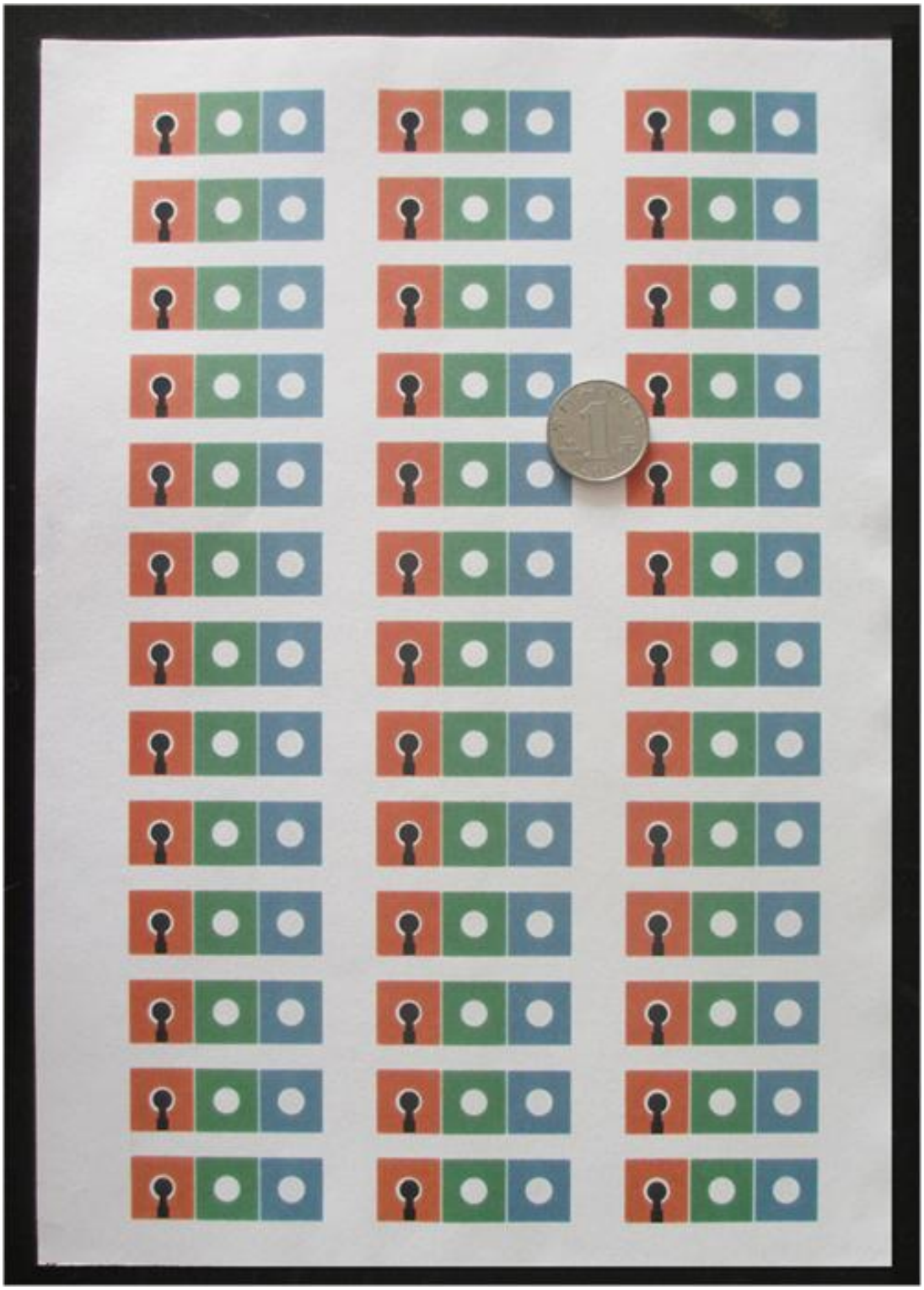

Figure S4. Right side of 3D-μ-OBFCADs on a paper sheet (A4) after screen-printing of carbon anodes.

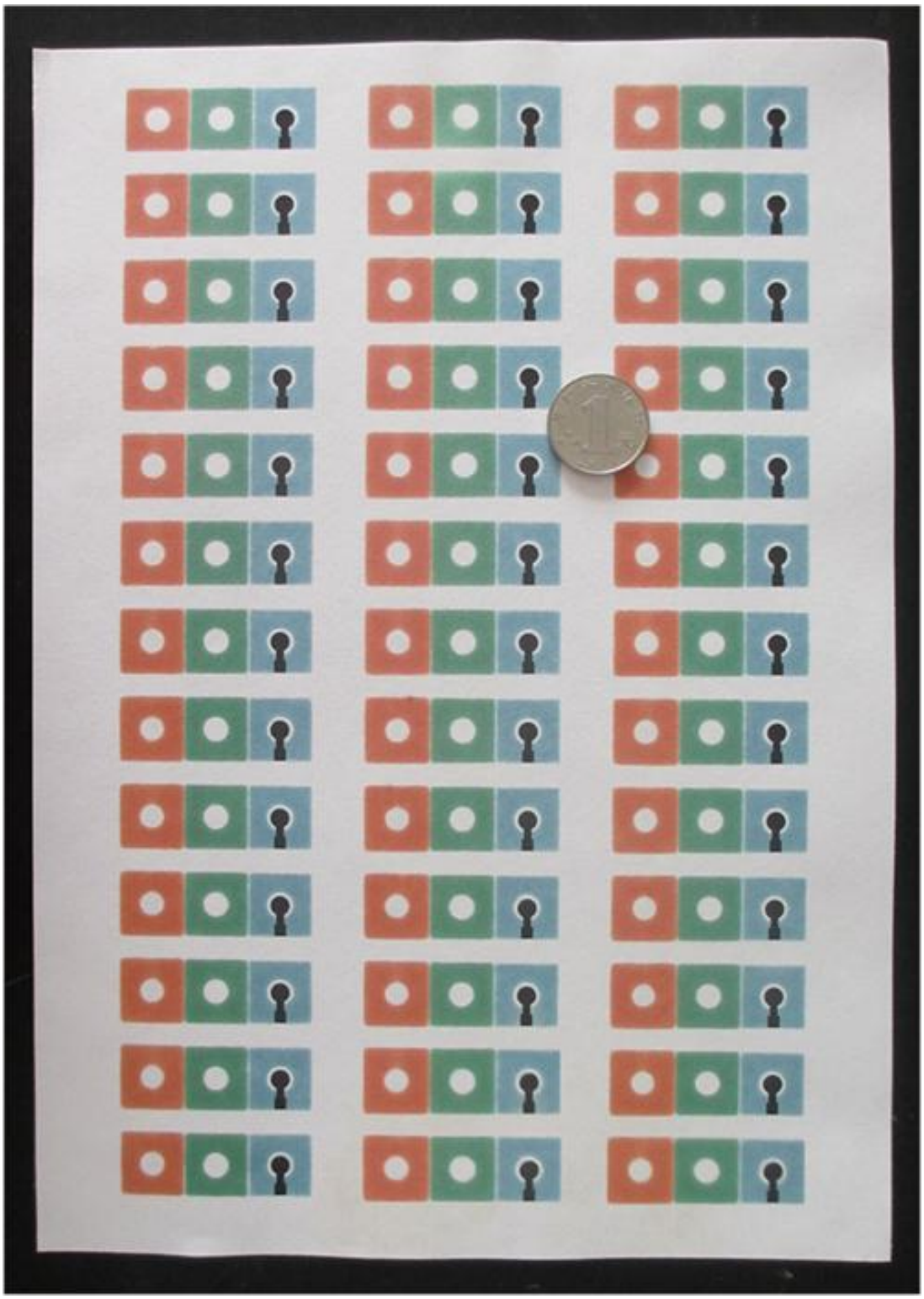

Figure S5. Reverse side of 3D-μ-OBFCADs on a paper sheet (A4) after screen-printing of carbon cathodes.

Construction of CNTs@AuNPs composites

The AuNPs (5 nm) were synthesized by the reduction of gold ions with sodium citrate [1]. In the preparations, all the glassware was cleaned in aquaregia (HCl/HNO_3=3:1), rinsed with triply ultrapure water, and oven-dried prior to use. $HAuCl_4$ (100 mL, 0.01 %) was heated to boiling under vigorous stirring, and trisodium citrate (1.5 mL, 1 %) was added with stirring. The solution turned blue within 25 s and the final color change to red or violet occurred 70 s later. Heating to boiling was continued for an additional 10 min, the heating source was removed, and the colloid was stirred for another 15 min. The solution was allowed to cool to room temperature. The obtained AuNPs were stored at 4 ℃ prior to use.

The CNTs@AuNPs was synthesized according to previous work [2]. The template of CNTs was first treated with 3:1 H_2SO_4/HNO_3 in sonication for 4 h. The resulting dispersion was filtered and washed repeatedly with water until pH was about 7.0. This procedure shortened CNTs, removed metallic and carbonaceous impurities, and generated carboxylate groups on the CNTs surface. Next, 0.5 mg/mL of the carboxylated CNTs was dispersed into a 0.20% PDDA aqueous solution containing 0.5 M NaCl by 30 min sonication to give a homogeneous black suspension. Residual PDDA polymer was removed by high-speed centrifugation, and the complex was thrice washed with water to obtain PDDA-functionalized CNTs. Then, the PDDA-functionalized CNTs (0.75 mg) were dispersed in 9.0 mL of as-prepared colloidal AuNPs and stirred for 20 min. After centrifugation, light purple CNTs@AuNPs composites were obtained, which were further washed with water and redispersed in 2.5 mL of 50 mM pH 9.0 Tris-HCl solutions.

Preparation of GDH-CNTs@AuNPs-Ab2 bioconjugate

The bioconjugates were freshly prepared by addition of Ab2 (500 $\mu g \cdot mL^{-1}$, 40 μL) and GDH

(10 μg·mL^{-1}, 100 μL) in PBS (0.01 M, pH 7.4) into CNTs@AuNPs nanoparticles solution (1.0 mL). The mixture was incubated at room temperature with gentle mixing for 2 h, and then the obtained GDH-CNTs@AuNPs-Ab2 bioconjugate were centrifuged and redispersed in 5 mL of 1% bovine serum albumin (BSA) solution containing 0.05% Tween for 2 h under stirring to block the excess amino group and nonspecific binding sites of the GDH-CNTs@AuNPs-Ab2 bioconjugate. Thereafter, the solution was centrifuged for 15 min at 15 000 rpm, and the supernatant was removed. Followed by washing with PBS (0.01 M, pH 7.4) for further purification and separated as above. The resulting {Ab2-CNTs@AuNPs-GDH} bioconjugates were redispersed in PBS, and were stored at 4 ℃prior to use.

Construction of bioanode and biocathode of the 3D-μ-OBFCAD

The Au-PAE/PCE was fabricated through growth of an AuNPs layer on the surfaces of cellulose fibers in the hydrophilic zone on anodic tab and cathodic tab to enhance the conductivity and enlarge the effective surface area of bare PAE/PCE (Scheme S2A-B). The porous Au-PAE/PCE was fabricated according to our previous work [4] and the procedures of the were described as follows: The suspension of AuNP seeds was prepared by using $NaBH_4$ as reductant and stabilized with sodium citrate according to the literature [5]. Then, as-prepared AuNP seeds solution (20.0 μL) was dropped into the hydrophilic zone on anodic tab and cathodic tab, respectively (Scheme S2A). Then the origami device was equilibrated at room temperature for 1 h to optimize the surface immobilization of Au NP seeds on cellulose fibers. After rinsing with water thoroughly according to the method in our previous work [6] to remove loosely bound Au NP seeds, freshly prepared growth aqueous solution (15 μL) of phosphate buffer (0.01 M, pH 7.0) containing $HAuCl_4$ (1.2×10^{-3} M), cetyltrimethylammonium chloride (2×10^{-3} M), and H_2O_2

(7.2×10^{-3} M) for seeds growth was applied into the AuNPs seeded PAE/PCE, respectively, and incubated at room temperature for 10 min. During the growth process, the Au NP seeds acted as catalysts for the reduction of $AuCl^{4-}$ by H_2O_2, resulting in the enlargement of the AuNP seeds [7]. Subsequently, the resulting porous Au-PAE/PCE was washed with water thoroughly. Thus a layer of interconnected AuNPs on cellulose fibers with good conductivity were obtained (Scheme S2B), and dried at room temperature for 20 min. The Scanning Electron Microscope (SEM) images of the μ-PADs and porous Au-PAE/PCE were recorded on a JEOL JSM-5510 scanning electron microscope. Transmission Electron Microscopy (TEM) investigations were performed using JEOL 4000 EX microscope. Electrochemical Impedance Spectroscopy (EIS) was performed on an IM6x electrochemical working station (Zahner Co., Germany).

The bianode of the 3D-μ-OBFCAD was constructed by immobilizing the capture antibodies (Ab1) on the AuNPs layer through the interaction between amino on Ab1 and Au NPs on Au-PAE. Briefly, 20 μL Ab1 was dropped into the porous Au-PAE and kept it for 1 h at room tempreture (Scheme S2C). Afterwards, they were rinsed with PBS (pH 7.4) to remove physically absorbed Ab1 and blocked with 10 μL 1% BSA solution containing 0.05% Tween for 30 min at room temperature to prevent possible remaining active sites against non-specific adsorption (Scheme S2E). While the biocathode was fabricated by spreading 20 μL of BOD (dissolved in 0.1 M pH 7.0 PBS) on the porous Au-PCE (Scheme S2D). After drying bioanode and biocathode at 4 ℃ overnight, the 3D-μ-OBFCAD was obtained.

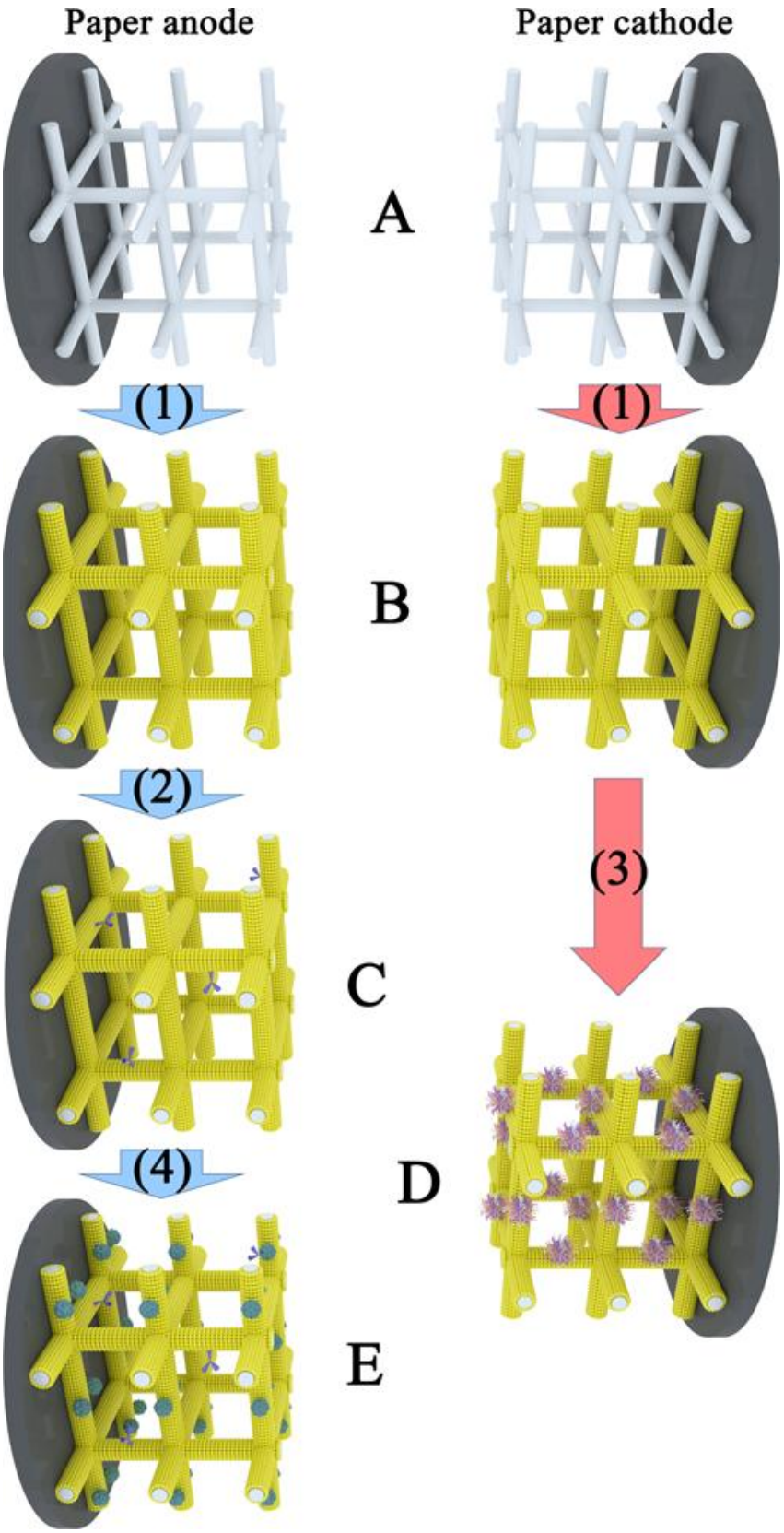

Scheme S2. Schematic diagram of the fabrication of the 3D-μ-OBFCAD. A) bare PAE/PCE; B) growth of a AuNP layer on the surfaces of cellulose fibers in bare PAE/PCE; C) immobilization of Ab1 in Au-PAE; D) immobilization of BOD in Au-PCE; E) blocking of Au-PAE by BSA.

Assay procedure of the 3D-μ-OBFCAD for users

The detail assay procedures of this 3D-μ-OBFCAD for users were shown in Scheme S3 and described as below. Briefly, first, sample solutions (20 μL) contained different concentrations of CEA was added into the bioanode (Scheme S3A) and allowed to incubate for 30 min at room temperature followed by washing thoroughly with PBS. Thereafter, 20 μL {Ab2-CNTs@AuNPs-GDH} bioconjugate were added into the bioanode and allowed to incubate for 30 min at room temperature (Scheme S3B). After washing with washing buffer again, 10 μL 0.10 M PBS (pH 7.0) was added to the hydrophilic zone of reservoir tab and cathodic tab to prewet them, respectively. Then, this 3D-μ-OBFCAD was immediately folded as indicated in Scheme S3C and was sequentially clamped by a home-made device folder to ensure contact (Scheme S3D). Finally, 20 μL 0.1 M pH 7.0 PBS containing 10 mM NAD^+/NADH and 30 mM glucose was added into to the Au-PAE through the hole on the device folder (Scheme S3D) to activate this 3D-μ-OBFCAD. The output current was recorded by the electrochemical workstation (Shanghai CH Instruments Co., China), and the concentration of CEA could be quantified by the peak current intensity.

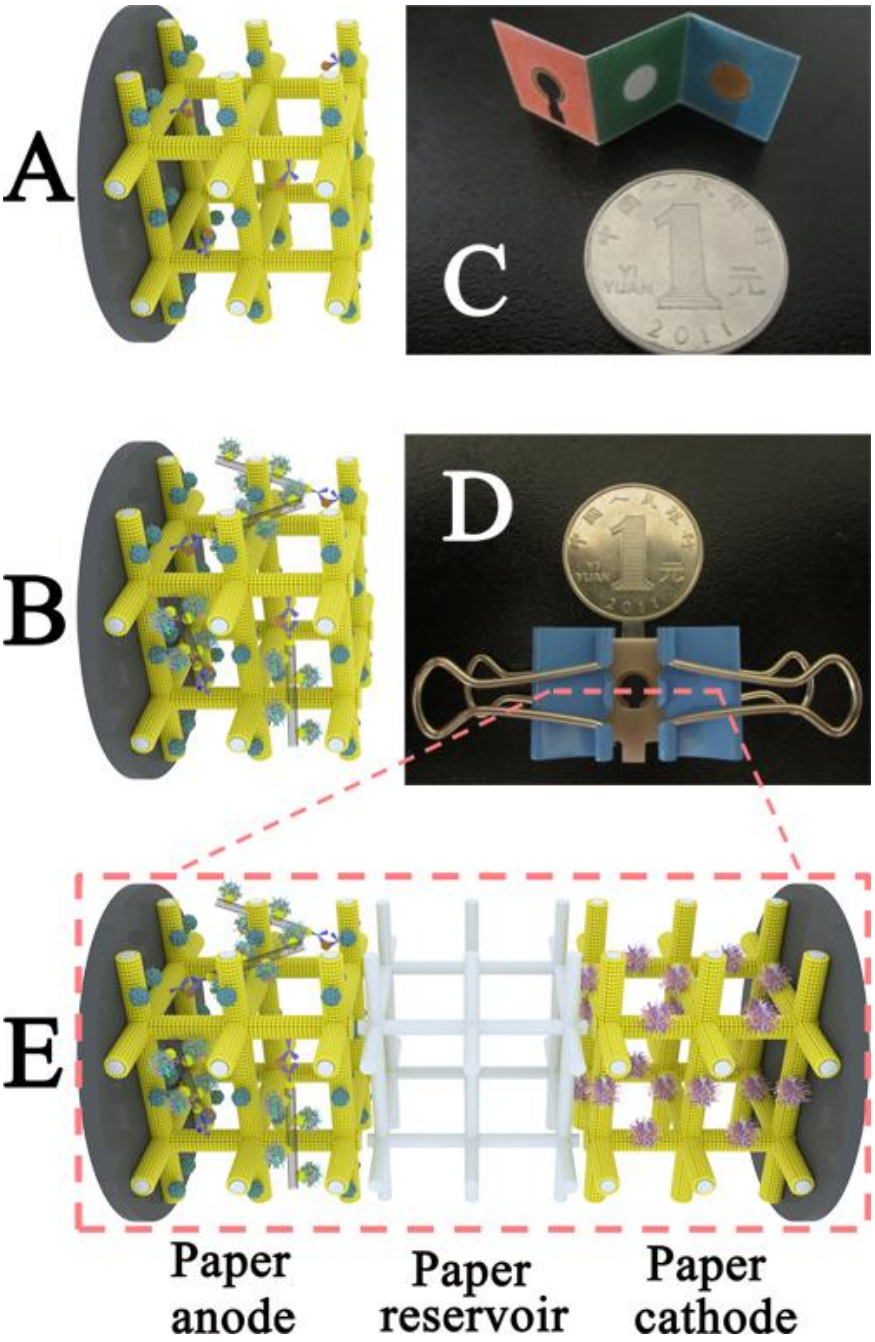

Scheme S3. Schematic representation of the assay procedure for this 3D-μ-OBFCAD. A) after capturing of CEA in the bioanode and washing; B) after incubation with labeled Ab2 to form Ab1/CEA/Ab2 sandwich immunocomplexes; C) picture of the folded 3D-μ-OBFCAD; D) the folded 3D-μ-OBFCAD was clamped by a home-made device folder; E) section view of this 3D-μ-OBFCAD after clamping.

Characterization of the Au NPs, CNTs@AuNPs, GDH-CNTs@AuNPs-Ab2 Bioconjugate and Au-PAE/PCE

TEM was employed to characterize the bare AuNPs, the TEM image (Figure S6A) revealed good monodispersity of the AuNPs, and the size was about 5.0 nm. The carboxylated CNTs showed a homogeneous surface and good dispersion (Figure S6B). After positively charged PDDA-modified CNTs were formed, the assembly of negatively charged AuNPs appeared larger in size and showed a distinctively more densely packed morphology (Figure S6C). The AuNPs could compactly and uniformly attach on the surface of the CNTs through the PDDA. The uniformly distributed AuNPs could selectively attach protein molecules for the biofunctionalization of the CNTs [8].

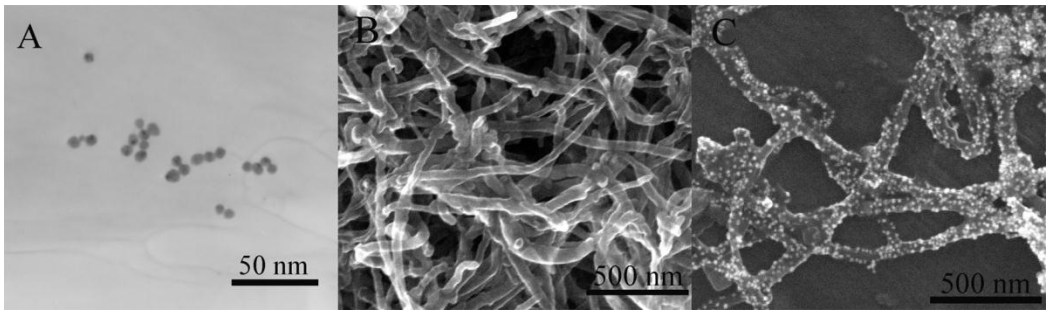

Figure S6 (A) the TEM images of AuNPs. (B) the SEM images of CNTs. (C) the SEM images of CNT@AuNPs.

As shown in Figure S7A, the porous bare hydrophilic zone, possessed high ratio of surface area to weight with rough cellulose fibers, could offer an excellent adsorption microenvironment for the AuNP seeds. It can be seen that there was no apparent structural and surface difference between the bare (Figure S7A) and the AuNPs seeded (Figure S7B) cellulose fibers in the paper sample zone of PAE/PCE due to the small particle size the small particle size of AuNP seeds (Figure S6A). The growth process of the Au NPs layer on the surface of Au NPs seeded cellulose fibers was confirmed by scanning electron microscopy (SEM) (Figure S7C). A continuous and

dense conducting AuNPs layer with interconnected Au NPs was obtained completely on the cellulose fiber surfaces after 10 min of growth.

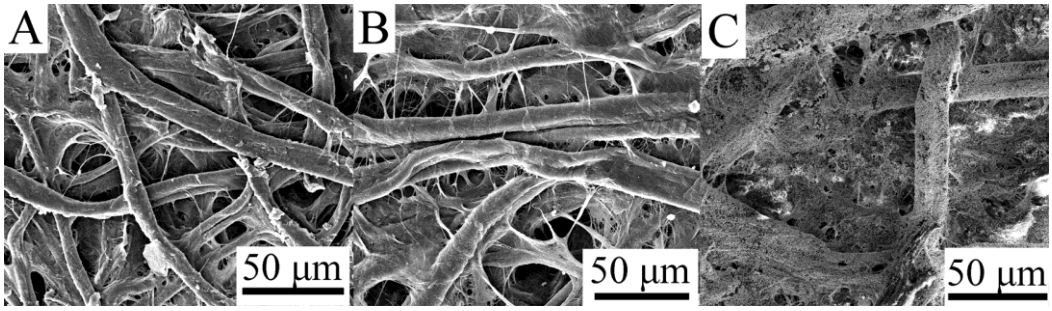

Figure S7. (A) the SEM image of bare paper electrode, (B) AuNP seeded paper electrode, (C) AuNPs on the surfaces of cellulose fibers in hydrophilic zone.

Electrochemical Characterization of Au-PAE/PCE

The electrochemical properties of the resulted Au-PAE/PCE under different condition were investigated through cyclic voltammetry (CV) toward 10.0 mM $[Fe(CN)_6]^{3-/4-}$ solution containing 0.5 M KCl. As shown in Figure S8, the bare PAE/PCE exhibited one set of well defined redox peaks toward $[Fe(CN)_6]^{3-/4-}$ (Curve a). For the Au-PAE/PCE, there was a sharp increase of the peak current (Curve b). The CV curves showed that the Au-PAE/PCE had a significant higher peak current and larger CV area compared with the bare one, indicating that the porous Au-PAE/PCE had a much larger effective surface area, which may be attributed to the high effective surface area of the AuNP layer on cellulose fibers and the porous morphology of paper.

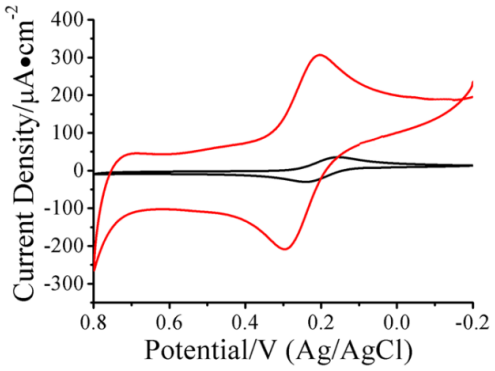

Figure S8. CVs of (a) bare PAE/PCE and (b) porous Au-PAE/PCE.

Electrochemical Characterization of bioanode/biocathode

Electrochemical impedance spectroscopy (EIS) of the resulting bioanode/biocathode could also give detail information about the modification process. Electrochemical impedances of bioanode/biocathode were performed in a background solution of 5.0 mM $[Fe(CN)_6]^{3-/4-}$ solution containing 0.5 M KCl,. In EIS, the diameter of the semicircle at higher frequencies corresponds to the electron-transfer resistance (Ret); a change in the value of Ret was associated with the blocking behavior of the modification processes in the porous Au-PAE, and was reflected in the EIS as a change in the diameter of the semicircle at high frequencies. Figure S9A showed the EIS (presented in the form of the Nyquist plot) of different surface conditions of the bioanade. The EIS of bare PAE revealed a relatively small semicircle domain (curve a). After the formation of Au-PAE, the EIS exhibited an obvious decrease in Ret (curve b). Remarkable increase in the Ret value was observed after the addition of Ab1 (curve c) into Au-PAE, suggesting that Ab1 were successfully immobilized on the surface and blocked the electron exchange between the redox probe and the electrode. Then, the Ret continue increased after BSA and CEA were immobilized onto Au-PAE gradually (curve d and e). At last, when {Ab2-CNTs@AuNPs-GDH} bioconjugate was added into the modified Au-PAE, the electron-transfer kinetics of the redox probe was slow down further (curve f), indicating that the nonconductive properties of biomacromolecule acted as a definite kinetic barrier for the charge transfer. For the biocathode, after the immobilization of BOD in porous Au-PCE, remarkable increase in the Ret value was observed (Figure S9B), indicated that the successful immobilization of BOD on porous Au-PCE [9].

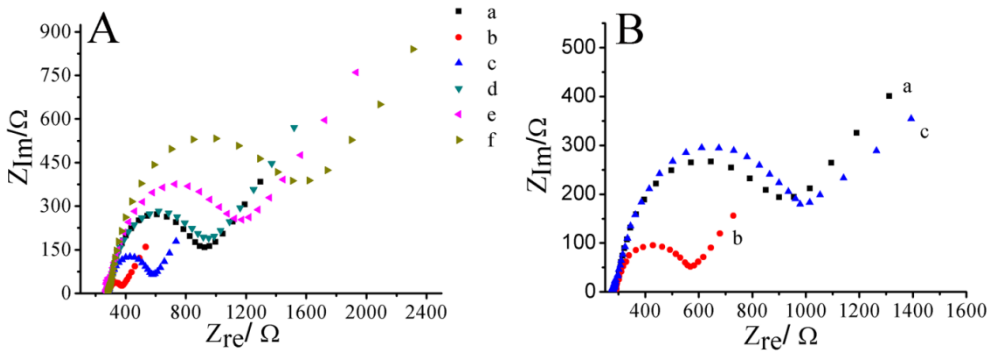

Figure S9. (A) EIS of the bioanode under different condition in 10.0 mM $[Fe(CN)_6]^{3+/4+}$ solution containing 0.5 M KCl. a) bare PAE, b) Au-PAE, c) Ab1 modified Au-PAE, d) after the absorption of BSA, e) after the addition of CEA, f) after the conjunction of {Ab2-CNTs@AuNPs-GDH}; (B) EIS of the Au-PCE under different condition in 10.0 mM $[Fe(CN)_6]^{3+/4+}$ solution containing 0.5 M KCl. a) bare PCE, b) Au-PCE, c) after the immobilization of BOD.

Optimization of the conditions

For paper-based point-of-care testing, the analytical cost, sensitivity and time efficiency is very important. The optimization procedures were performed at room temperature and consistent to the assay procedures. The effects of incubation time on the current intensity of this 3D-μ-OBFCAD were investigated as follows. With the increasing of incubation time for CEA capture and Ab2 incubation, the output current intensities for 100 nM CEA increased quickly and have reached maximum values at 30 min (Figure S10A), indicating the maximum formation of the sandwich immunecomplexe. Thus, an incubation time of 30 min was selected in the further study. In this work, the glucose was used as the fuel oxidized by GDH, and the concentration of glucose could influence the current intensity. Thus, the generated current was optimized by changing the concentration of glucose. As shown in Figure 2B, when the concentration of glucose was lower than 30 mM, the current increased with increasing glucose concentration; when the concentration of glucose was higher than 30 mM, the current intensity did not increase obviously. Therefore, 30 mM glucose was used in this work. To achieve an optimal current signal, the pH value of the substrate solution was the important factor to the current intensity of this 3D-μ-OBFCAD. The

current intensity was measured from 5.0 to 9.0 containing 100 nM CEA, and the maximum was observed at pH 7.0. The reason was that the high acidic or alkaline surroundings would damage the immobilized protein [10]. Since the optimal pH value for the biological systems was 7.0, the detection of this 3D-μ-OBFCAD was performed in pH 7.0 PBS containing containing 10 mM NADH/NAD^+ and 30 mM glucose.

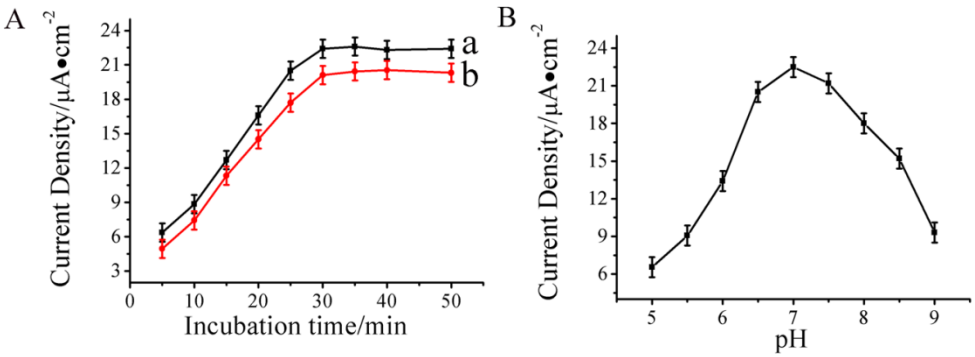

Figure S10. (A) The effect of incubation time on current intensity at 100 nM CEA concentration. a) Incubation time between CEA and Ab2, b) Incubation time between Ab1 and CEA. (B) Effect of pH value on current intensity.

Analytical performance

Compared with other CEA assays reported in the literatures (Table S1), the proposed 3D-μ-OBFCAD had a relative large linear range and low detection limit. Meanwhile, the analytical reliability and application potential of this 3D-μ-OBFCAD was evaluated by assaying clinical serum samples using the proposed method as well as the reference values obtained by commercially used electrochemiluminescence (ECL) method in Cancer Research Center of Shandong Tumor Hospital. When the levels of tumor markers were over the calibration ranges, serum samples were appropriately diluted with 10.0 mM pH 7.4 PBS prior to assay. The results were shown in Table S2, the results gave the relative errors less than 5.7% for CEA, showing an acceptable agreement. Hence, the developed 3D-μ-OBFCAD provided a possible application for

the detection of CEA in clinical diagnosis.

Table S1. Comparison of analytical properties of different immunoassys toward CEA.

Immunoassay format	Linear range (ng mL^{-1})	Detection limit (pg mL^{-1})	References
Electrochemical	0.5-120	400	[11]
Electrochemiluminescence	1.0-100	500	[12]
Electrochemical	0.0025-2	1.4	[13]
Electrochemical	0.01-160	5	[14]
Electrochemical	0.001-1000	0.85	This work

Table S2. Assay results of real human serum by the proposed and reference method.

Samples	CEA concentration (ng·mL^{-1})		
	Proposed method[a]	Reference method[a]	Relative error (%)
Sample-1	21.3	20.1	5.63
Sample-2	35.8	37.1	-3.63
Sample-3	53.1	50.7	4.52
Sample-4	82.3	79.2	3.77

[a] Average of eleven measurements.

Specificity, Reproducibility, and Stability of this 3D-μ-OBFCAD

To verify the specificity of this 3D-μ-OBFCAD for CEA detection, experiments were performed by using some structurally related interference in human serum, such as prostate specific antigen (PSA), fetoprotein (AFP), human chorionic gonadotrophin (HCG) and human

serum albumin (HSA). The current responses to each type of antigen (100 nM) were recorded in Figure S11. The interference degree of variability between different tumor markers was acceptable.

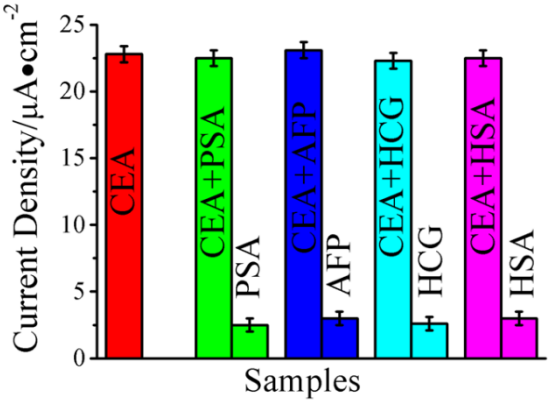

Figure S11. Selectivity of the proposed 3D-μ-OBFCAD (CEA, PSA, HCG, AFP, HSA, 100 nM).

The reproducibility of the 3D-μ-OBFCAD was investigated based on interassay precision between 10 3D-μ-OBFCAD (measurements of the same sample on 10 different 3D-μ-OBFCAD prepared in different batches). The RSDs for the parallel detection of 0, 10.0, and 50.0 pM CEA with 10 3D-μPADs, respectively, were 3.58%, 3.72%, and 3.64%. To investigate the stability of this 3D-μ-OBFCAD, it was stored at 4 ℃ and measured at intervals of 3 days; no obvious change was observed after 4 weeks. These results indicated that this 3D-μ-OBFCAD had good reproducibility and was fairly robust in normal storage conditions and achieved sufficient stability and precision during manufacture, storage, or long-distance transport to remote regions and developing countries.

Reference

1 K. C. Grabar, R. G. Freeman, M. B. Hommer and M. J. Natan, Anal. Chem. 1995, 67, 735–743.

2 H.Y. Liu, S.M. Xu, Z.M. He, A.P. Deng and J.J. Zhu, Anal. Chem., 2013, 85, 3385–3392.

3 J.X. Yan, M. Yan, L. Ge, J.H. Yu, S.G. Ge and J.D. Huang, Chem. Commun., 2013,49, 1383-1385.

4 L. Ge , S.M. Wang, J.H. Yu, N.Q. Li, S.G. Ge and M. Yan, Adv. Funct. Mater., 2013, 23, 3115–3123.

5 B. D. Busbee, S. O. Obare, C. J. Murphy, Adv. Mater. 2003, 15, 414-416.

6 J.X. Yan, L. Ge, X.R. Song, M. Yan, S.G. Ge and J.H. Yu, Chem. Eur. J., 2012, 18, 4938-4945.

7 M. Zayats, R. Baron, I. Popov, I. Willner, Nano Lett. 2005, 5, 21-25.

8 K. Jiang, A. Eitan, L.S. Schadler, P.M. Ajayan, R.W. Siegel, N. Grobert, M. Mayne, M. Reyes-Reyes, H. Terrones, and M. Terrones, Nano Lett. 2003, 3, 275–277.

9 A. Korani, A. Salimi, Biosens. Bioelectron., 2013, 50, 186–193.

10 R. Yuan, D. P. Tang, Y. Q. Chai, X. Zhong, Y. Liu and J. Y. Dai, Langmuir, 2004, 20, 7240-7245.

11 F. Tan, F. Yan, and H.X. Ju, Electrochem. Commun. 2006, 8, 1835–1839.

12 L. Ge, J.X. Yan, X.R. Song, M. Yan M, S.G. Ge, and J.H. Yu, Biomaterials, 2012, 33, 1024–1031.

13 G.S. Lai, F. Yan F, and J.H. Ju, Anal. Chem., 2009, 81, 9730–9736.

14 D.P. Tang, R. Yuan, and Y.Q. Chai, Anal. Chem., 2008, 80, 1582–1588.